MHD Natural Convection Flow of Tangent Hyperbolic Nanofluid Past a Vertical Permeable Cone

A. Mahdy

Abstract—In this paper, a non-similraity analysis has been presented to exhibit the two-dimensional boundary layer flow of magnetohydrodynamic (MHD) natural convection of tangent hyperbolic nanofluid nearby a vertical permeable cone in the presence of variable wall temperature impact. The mutated boundary layer nonlinear governing equations are solved numerically by the an efficient implicit finite difference procedure. For both nanofluid effective viscosity and nanofluid thermal conductivity, a number of experimental relations have been recognized. For characterizing the nanofluid, the compatible nanoparticle volume fraction model has been used. Nusselt number and skin friction coefficient are calculated for some values of Weissenberg number W, surface temperature exponent n, magnetic field parameter M_g, power law index m and Prandtl number Pr as functions of suction parameter. The rate of heat transfer from a vertical permeable cone in a regular fluid is less than that in nanofluids. A best convection has been presented by Copper nanoparticle among all the used nanoparticles.

Keywords—Tangent hyperbolic nanofluid, finite difference, non-similarity, isothermal cone.

I. INTRODUCTION

NANOFLUID represents an innovative class of heat transfer fluid. Nanofluid is described as a combination of nanoparticles with the length scales of $1 - 100$ nm and the regular fluid. Choi [1] in 1995 presented an innovative technique, that used a mixture of regular fluid and nanoparticles for enhancing advanced heat transfer fluids with higher conductivities. Choi pointed out the resulting mixture as a nanofluid. To save the energy, the heat transfer enhances are needful in the evolution and manufacturing of electronic devices. Due to this requirement, in recent years, a number of researchers have been focused on addressing the nanofluid. Cheng [2] reported the natural convection boundary layer nanofluid flow through a porous horizontal cylinder of elliptic cross section. The laminar natural convection past a vertical wavy surface immersed in a porous medium saturated with a nanofluid was examined by Mahdy and Ahmed [3]. The single nanoparticle impact on the contact line motion was addressed by Li et al. [4]. The authors obtained three types of contact line motion involving complete slipping, alternate pinning-depinning, and complete pinning, and theoretically illustrated them. There are two sorts allow to incorporate nanoparticle aspect on fluid flow, namely single-phase nanofluid model as Sarkar [5] and two-phase nanofluid model as Buongiorno [6] Contributions

Mahdy is with the Department of Mathematics, Faculty of Science, South Valley University, Qena, Egypt (e-mail: mahdy@svu.edu.eg).

of both theoretical and experimental on nanofluid heat transfer properties are pointed out [7]-[17].

Non-Newtonian liquids' salient properties have been examined substantially by many researchers due to its wide existence in different industrial and technological applications. Non-Newtonian materials characteristics related to their shear stress behavior which are not denoted by a single constitutive relationship. With slip conditions and Joule heating, the impacts of MHD on peristaltic flow of hyperbolic tangent nanofluid in an inclined channel is explored by Hayat et al. [18]. Hayat et al. [19] reported the characteristics of magnetic field and melting heat transfer flow of tangent hyperbolic fluid in stagnation point. Shehzad et al. [20] examined the impact of magnetic field in three-dimensional flow of an Oldroyd-B nanofluid past a radiative surface. Waqas et al. [21] addressed the generalized Burgers fluid associated with model of Cattaneo-Christov heat flux. Abbas et al. [22] addressed three dimensional peristaltic hyperbolic tangent fluid flow in non-uniform channel with flexible walls. Ibrahim et al. [23] addressed the problem of non-Darcy free and forced convection of a non-Newtonian fluid from an isothermal vertical plate in the existence of surface injection or suction. Mahdy [24] exhibited non-Newtonian nanofluid natural convection flow associated with mixed thermal boundary conditions past a vertical cone. Similarity solutions have been presented for non-Newtonian natural convection flow over horizontal cylinder and a sphere in porous media by Chen and Chen [25, 26]. An analysis is performed to investigate the impact of heat generation and absorption on tangent hyperbolic nanofluid near the stagnation point over a stretched cylinder by Salahuddin et al. [27]. Ramesh et al. [28] exhibited stagnation point of Maxwell nanofluid flow along permeable stretching surface. A comprehensive review for the boundary layer natural convection flow towards cones [29]-[32], Cheng [33] presented a numerical solution for free convection boundary layer micropolar fluid flow over a permeable vertical cone with non-uniform heating surface. Postelnicu [34] examined the natural convection of a micropolar fluid past a vertical frustum of a cone.

The major purpose of this article is to exhibit the MHD natural convection boundary layer flow towards an isothermal vertical permeable cone in tangent hyperbolic nanofluid. A convenient non-similar transformations are invoked to mutate the governing boundary layer equations into a non-similar form. The finite difference procedure is chosen to get the
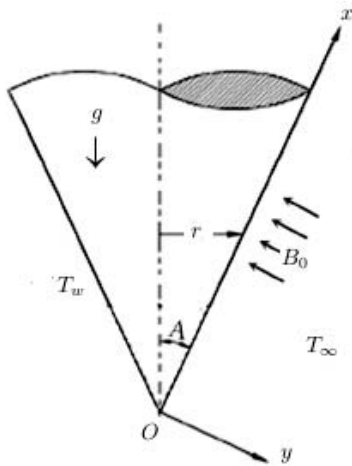
World Academy of Science, Engineering and Technology
International Journal of Aerospace and Mechanical Engineering
Vol:13, No:9, 2019

Fig. 1 Sketch of problem geometry

numerical solution of the resulting system.

II. MATHEMATICAL MODEL

Let us exhibit two-dimensional, steady, MHD free convection boundary layer flow of a tangent hyperbolic nanofluid nearby a permeable vertical cone considering variable wall temperature. The coordinate system origin is positioned at the vertex of the isothermal cone ($x = 0$), with x is the cone surface coordinate that measured from the origin and y is the coordinate normal to the cone surface as sketched in Fig. 1. The surface of the permeable cone is held at a mutable temperature $T_w(x)$ which is greater than the ambient fluid temperature T_∞, i.e $T_w > T_\infty$. A magnetic field with uniform strength B_0 is applied in y-direction, i.e, normal to flow direction. The magnetic Reynolds number is assumed to be petty and thus the induced magnetic field has been ignored. The aspect both of Hall and electric field have been neglected. With Boussinesq approximations help, the governing equations for the present model flow can be formulated as:

$$\frac{\partial(ru)}{\partial x} + \frac{\partial(rv)}{\partial y} = 0 \qquad (1)$$

$$\rho_{nf}\left(u\frac{\partial u}{\partial x} + v\frac{\partial u}{\partial y}\right) = \mu_{nf}(1-m)\frac{\partial^2 u}{\partial y^2} - \sigma_{nf}B_0^2 u +$$
$$\sqrt{2}\, m\mu_{nf}\gamma\left(\frac{\partial u}{\partial y}\right)\frac{\partial^2 u}{\partial y^2} + g(\rho\beta)_{nf}(T - T_\infty)\cos A \quad (2)$$

$$(\rho c_p)_{nf}\left(u\frac{\partial T}{\partial x} + v\frac{\partial T}{\partial y}\right) = k_{nf}\frac{\partial^2 T}{\partial y^2} \qquad (3)$$

subjected to the compatible boundary conditions at the cone surface and far away from it

$$u(x,0) = v(x,0) + V_w = 0, \quad T(x,0) = T_w = T_\infty + ax^n$$
$$u(x,\infty) \rightarrow 0, \qquad T(x,\infty) \rightarrow T_\infty \qquad (4)$$

We denoted by u, v to the nanofluid velocity components in x and y directions, respectively, r represents the radius of the cone, μ_{nf}, ρ_{nf}, k_{nf}, σ_{nf} and $(c_P)_{nf}$ point out nanofluid

TABLE I
THE NANOFLUID EFFECTIVE VISCOSITY AND THERMAL CONDUCTIVITY

Nano.	μ_{nf}/μ_f	k_{nf}/k_f
Cu [40]	$(1-\varphi)^{-5/2}$	$\frac{k_p+2k_f+2.662\varphi(k_p-k_f)}{k_p+2k_f-2.662\varphi(k_p-k_f)}$
Al$_2$O$_3$ [38]	$1+39.11\varphi+533.9\varphi^2$	$1+7.47\varphi$
Ag [39]	$1.005+0.497\varphi-0.1149\varphi^2$	$0.9508+0.9692\varphi$
TiO$_2$ [38]	$1+5.45\varphi+108.2\varphi^2$	$1+2.92\varphi-11.99\varphi^2$

viscosity, nanofluid density, nanofluid thermal conductivity, effective electrical conductivity and specific heat at constant pressure, β_{nf} gives the expansion effective thermal volumetric coefficient, m refers to the power law index, γ is the time dependent material constant. the half angle of the cone is denoted by A. In addition, V_w represents the suction velocity, a indicates a constant, and n refers to the power law of surface temperature. We present the stream function $\psi(x,y)$ which leads to the continuity equation (1) be satisfied as $u = r^{-1}\partial\psi/\partial y$ and $v = -r^{-1}\partial\psi/\partial x$. As the radius of the cone is relatively large compared with the thickness of boundary layer, then the local radius to a point inside the region of boundary layer can be determined by $r = x\sin A$.

Now, the relations that characterize the effective properties of nanofluid are given as

$$\rho_{nf} = (1-\varphi)\rho_f + \varphi\rho_p,$$
$$(\rho c_p)_{nf} = (1-\varphi)(\rho c_p)_f + \varphi(\rho c_p)_p$$
$$(\rho\beta)_{nf} = (1-\varphi)(\rho\beta)_f + \varphi(\rho\beta)_p,$$
$$\sigma_{nf} = \sigma_f\left(1+\frac{3(\sigma-1)\varphi}{\sigma+2-(\sigma-1)\varphi}\right), \quad\left(\sigma = \frac{\sigma_p}{\sigma_f}\right)(5)$$

φ gives the volume fraction of nanoparticles, ρ_f and ρ_p represent density of base fluid and nanoparticles, $(c_p)_f$ and $(c_p)_p$ indicate specific heat of the base fluid and nanoparticles, σ_f and σ_p denote the electrical conductivity of base fluid and nanoparticles, β_f and β_p are thermal volumetric coefficient of the base fluid and nanoparticles respectively and k_f and k_s give thermal conductivity of base fluid and nanoparticles respectively. For each sort of nanoparticles, experimental relations for both the nanofluid thermal conductivity k_{nf} and the nanofluid effective viscosity μ_{nf} have been applied. These relations can be collected as listed in Table I. Again, the properties of thermo-physical of nanoparticles and water are presented clearly in Table II.

We present the following non-similarity transformation

$$\eta = \frac{y}{x}Gr^{1/4}, \quad \xi = V_w x/\left(\nu_f Gr^{1/4}\right),$$
$$\psi = r\nu_f Gr^{1/4}\left(F+\frac{1}{2}\xi\right), \theta = \frac{T-T_\infty}{T_w-T_\infty} \qquad (6)$$

Then the governing boundary layer equations, (2) and (3) can be reformulated as

$$\left(\frac{\mu_{nf}}{\mu_f}\right)\left((1-m)F''' + mWF''F'''\right) - \frac{\sigma_{nf}}{\sigma_f}M_g F' +$$
$$\frac{\rho_{nf}}{\rho_f}\left(\frac{n+7}{4}FF'' + \xi F'' - \frac{n+1}{2}F'^2\right) + \frac{(\rho\beta)_{nf}}{(\rho\beta)_f}\theta =$$
$$\frac{\rho_{nf}}{\rho_f}\frac{1-n}{4}\xi\left(F'\frac{\partial F'}{\partial\xi} - F''\frac{\partial F}{\partial\xi}\right) \qquad (7)$$

World Academy of Science, Engineering and Technology
International Journal of Aerospace and Mechanical Engineering
Vol:13, No:9, 2019

TABLE II
THERMO-PHYSICAL PROPERTIES OF WATER AND NANOPARTICLES [37]

	ρ	c_p	k	$\beta \times 10^5$	$\sigma \times 10^{-6}$
Cu	8933	385	401	1.67	59.6
Al$_2$O$_3$	3970	765	40	0.85	36.9
Ag	10500	235	429	1.89	63
TiO$_2$	4250	686.2	8.9538	0.90	2.4
H$_2$O	997.1	4179	0.6130	21	5.5$\times 10^{-12}$

$$\frac{1}{Pr}\frac{k_{nf}}{k_f}\theta'' + \frac{(\rho c_p)_{nf}}{(\rho c_p)_f}\left(\frac{n+7}{4}F\theta' - nF'\theta + \xi\theta'\right) =$$
$$\frac{(\rho c_p)_{nf}}{(\rho c_p)_f}\frac{1-n}{4}\xi\left(F'\frac{\partial\theta}{\partial\xi} - \theta\frac{\partial F'}{\partial\xi}\right) \qquad (8)$$

In addition, the convenient boundary conditions can be reformulated in dimensionless form as

$$F(\xi,0) = F'(\xi,0) = 0, \quad \theta(\xi,0) = 1$$
$$F'(x,\infty) \to 0, \qquad \theta(\xi,\infty) \to 0 \qquad (9)$$

the parameter $W = \frac{\sqrt{2}\mu_f\gamma Gr^{3/4}}{\rho_f x^2}$ gives the Weissenberg number, $Pr = \frac{\mu_f(c_p)_f}{k_f}$ refers to Prandtl number, $M_g = \frac{\sigma_f B_0^2 x^2}{\mu_f Gr^{1/2}}$ indicates the magnetic field parameter, $Gr = \frac{\rho_f^2 g\beta_f(T_w - T_\infty)x^3\cos A}{\mu_f^2}$ is the Grashof number and ξ means the suction parameter.

Now, skin friction coefficient and local Nusselt number represent the most important physical quantities and are given by

$$C_f = \frac{\tau_w}{\frac{1}{2}\rho_f U^2}, \qquad Nu = \frac{xq_w}{k_f(T_w - T_\infty)} \qquad (10)$$

U is a reference velocity, the quantities τ_w and q_w refer to the surface shear stress, and the local heat transfer rate per unit area of surface and are given by

$$\tau_w = \mu_{nf}\left((1-m)\frac{\partial u}{\partial y} + \frac{m\gamma}{\sqrt{2}}\left(\frac{\partial u}{\partial y}\right)^2\right)_{y=0},$$
$$q_w = -k_{nf}\left(\frac{\partial T}{\partial y}\right)_{y=0} \qquad (11)$$

In non-dimensional form the skin friction coefficient C_f and local Nusselt number Nu are formulated as

$$\frac{1}{2}Gr^{1/4}\,C_f = \frac{\mu_{nf}}{\mu_f}\left((1-m)F'' + \frac{mW}{2}F''^2\right)_{(\xi,0)},$$
$$Gr^{-1/4}\,Nu = -\frac{k_{nf}}{k_f}\theta'(\xi,0) \qquad (12)$$

III. RESULTS AND DISCUSSION

The finite difference method represents the used numerical algorithm to get the solution of the non-dimensional governing PDEs. Equations (7) and (8) related to the boundary conditions (9). To approximate the derivatives of the first and second orders of the dependent variables with respect to η, a formula of three-point central difference has been selected, whereas the formula of backward is chosen for the derivatives with respect to suction variable ξ. The resulted algebraic system has been solved considering the tri-diagonal matrix algorithm (TDMA).
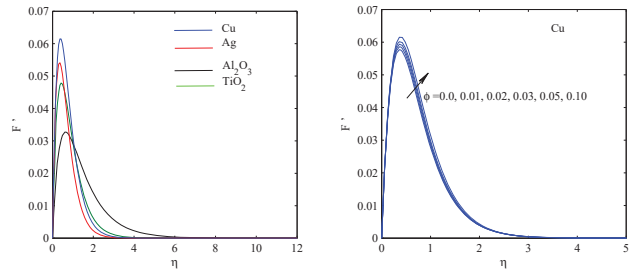

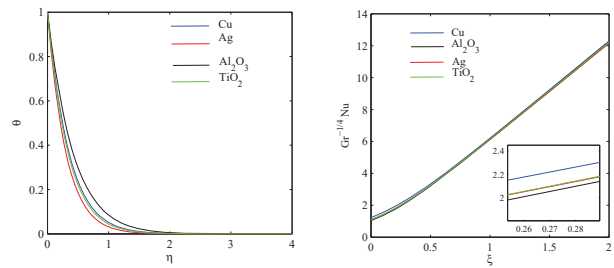Fig. 2 F' profiles with different types nanoparticles and φ

Fig. 3 Variation of θ and $Gr^{-1/4}Nu$ with nanoparticles

This procedure has been illustrated in detail by Blottner [36].

Now, in order to examine the accuracy of the present method, our obtained computations have been compared in particular cases with the previously published papers. For various values of suction variable ξ, Table III stands for a comparison of $Gr^{-1/4}Nu$ when $m = 0, n = 0.5, W = 0, Pr = 0.1$ and $\varphi = 0$. The table explains that the present results are in excellent agreement with the data obtained by Cheng [33] and Hossain and Paul [35]. Influence of
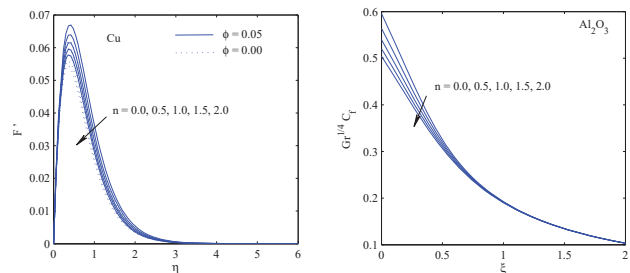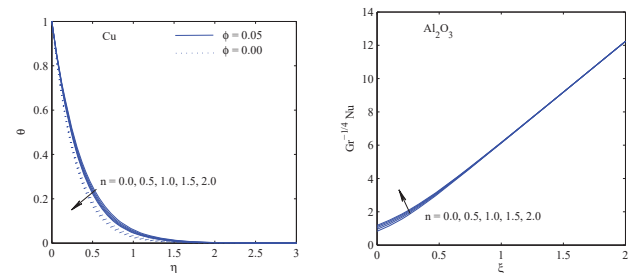

Fig. 4 Variation of F' and $Gr^{1/4}C_f$ against n

Fig. 5 Variation of θ and $Gr^{-1/4}Nu$ against n

World Academy of Science, Engineering and Technology
International Journal of Aerospace and Mechanical Engineering
Vol:13, No:9, 2019

different types of nanoparticles and solid volume fraction of nanoparticles φ on velocity F' profiles have been given in Fig. 2. As shown, Cu-nanoparticle leads to a large upgrade in the velocity profile with respect to the other types of nanoparticles. Hence, Cu-nanoparticle has the largest rate of fluid flow. The Al_2O_3 nanoparticle gives the lowest distribution of velocity behavior. In addition, as noticed the Ag-nanoparticle velocity profile is higher than the TiO_2-nanoparticle velocity profile. An increment in φ tends to enhance the velocity distribution. Unlike the behavior of velocity, the temperature curve in the case of Al_2O_3-nanoparticle leads to the largest value compared with the other nanoparticles, whilst the Ag-nanoparticle has the lowest one as seen in Fig. 3 which sketches the temperature curves and Nusselt number for some different types of nanoparticles. Again, the temperature distribution in the case of Cu-nanoparticle is higher than that of the TiO_2-nanoparticle. Moreover, Fig. 3 explores that Cu-nanoparticle has the highest value of the local Nusselt number $Gr^{-1/4}Nu$.

Figs. 4 and 5 illustrate the impact of surface temperature exponent parameter ($n = 0.0, 0.5, 1.0, 1.5$ and 2) with $W = 0.5, M_g = 1.0, Pr = 6.2$ and $m = 0.5$ for Cu and Al_2O_3 nanoparticles as $\varphi = 0.05$. Enlarging n parameter tends to upgrade the buoyancy force, then the flow is accelerated and therefore enhancing the local heat transfer rate $Gr^{-1/4}Nu$. As clear, the local Nusselt number tends to upgrade when the surface temperature exponent enlarges for small values of suction variable ξ and this behavior absent for large values of ξ, whereas an opposite behavior is happened with the skin friction coefficient Fig. 4, i.e. $Gr^{1/4}C_f$ downgrades with enlarging the surface temperature exponent. In addition, The impact of surface temperature exponent on velocity F' and temperature θ curves is given in Figs. 4 and 5. A clear reduction is happened for both of velocity and temperature curves.

The aspect of the nanoparticle solid volume friction φ on the temperature θ distribution and the local Nusselt number $Gr^{-1/4}Nu$ for the Cu-nanoparticle is given in Fig. 6. An upgrade in φ, all of θ and $Gr^{-1/4}Nu$ upgrade. Generally, the nanofluid thermal conductivity has an important role in such types of problems. Due to this point, the behaviors of θ and $Gr^{-1/4}Nu$ is significantly under the aspect of φ. Therefore, as φ enlarges, the nanofluid thermal conductivity upgrades which tends to a best convection. Magnetic field parameter M_g impact ($M_g = 0.0, 1.0, 2.0, 3.0$ and 5.0) with $W = 0.5, n = 1.0, Pr = 6.2$ and $m = 0.5$ for Al_2O_3 nanoparticle as $\varphi = 0.05$ is explored in Figs. 7 and 8. Variations As observed, magnetic field parameter leads to reduce the velocity profile whilst rise the temperature profiles. The plotted figures illustrate that both of the local Nusselt number and local skin friction coefficient tend to downgrade when the magnetic filed parameter is enlarged. Fig. 9 explains the impact of Weissenberg number on the velocity distribution and skin friction coefficient. The figure illustrates that an enlarge in Weissenberg number leads to reduce the velocity profile, but upgrade the skin friction coefficient.

The influence of power law index m on velocity profile and skin friction coefficient is plotted in Fig. 10. As m increases the skin friction coefficient downgrades. Rising m values leads
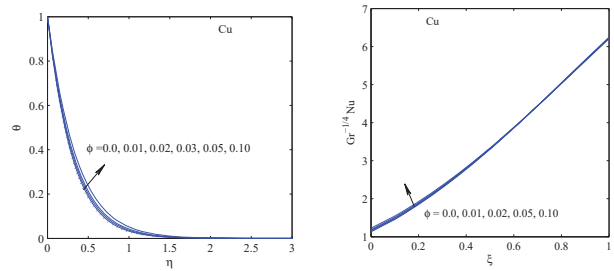

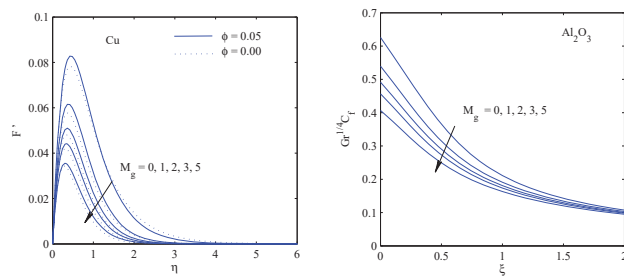Fig. 6 Variation of θ and $Gr^{-1/4}Nu$ against φ

Fig. 7 Variation of F' and $Gr^{1/4}C_f$ against M_g

to upgrade the velocity profile nearby the surface of the cone then the velocity reduces far away from the surface. Finally, the impact of suction parameter ξ on temperature and velocity profiles is plotted in Fig. 11. The figure displays that suction variable higher values make thinner thermal layer thickness, upgrading the temperature gradient at the wall cone and hence upgrade the rate of heat transfer. While, enlarging the suction variable leads to reduce the velocity profiles.
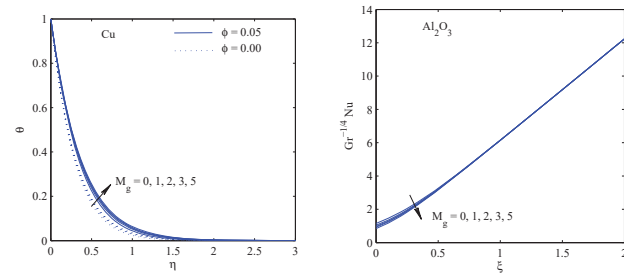

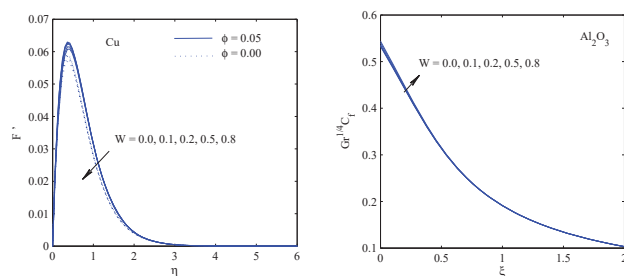Fig. 8 Variation of θ and $Gr^{-1/4}Nu$ against M_g
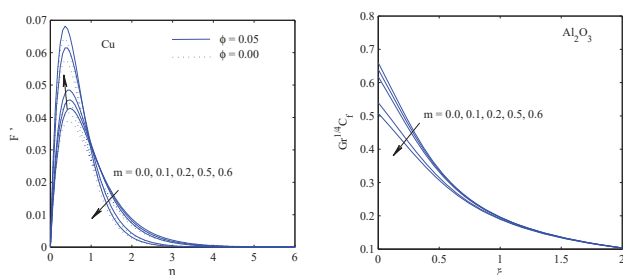

Fig. 9 Variation of F' and $Gr^{1/4}C_f$ against W

World Academy of Science, Engineering and Technology
International Journal of Aerospace and Mechanical Engineering
Vol:13, No:9, 2019

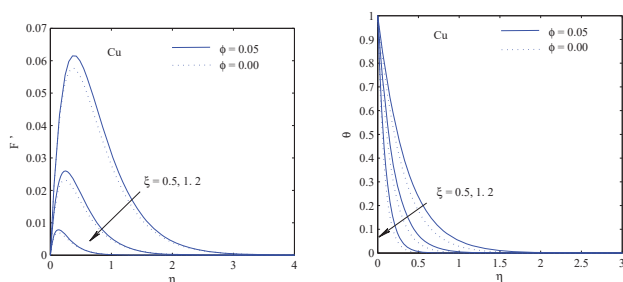Fig. 10 Variation of F' and $Gr^{1/4}C_f$ against m

Fig. 11 Variation of F' and θ against ξ

IV. CONCLUSION

MHD free convection boundary layer flow of a tangent hyperbolic nanofluid of a single-phase model over an isothermal vertical permeable cone has considered in the present article. A non-similar solution with the help of an implicit finite difference technique have been performed to solve the motion governing equations. For both the nanofluid effective viscosity and the nanofluid thermal conductivity, different experimental relations have been used with each sort of fluid. Results illustrate that Weissenberg number leads to downgrade the velocity profile and enhances the skin friction coefficient. Also, Cu-nanoparticle gives higher rates of heat transfer. In addition, an upgrade in the surface temperature exponent gives a reduction in velocity but, an upgrade local Nusselt number.

TABLE III
COMPARISON $-\theta'(0,0)$ VALUES FOR DIFFERENT VALUES OF ξ WITH $n = 0.5, Pr = 0.1$ AND $\varphi = 0$

	[33]	[35]	Present
0.0	0.2460	0.24584	0.245954
0.1	0.2509	0.25089	0.250936
0.2	0.2559	0.25601	0.255926
0.4	0.2660	0.26630	0.265941
0.6	0.2760	0.27662	0.276019
0.8	0.2862	0.28694	0.286180
1.0	0.2965	0.29731	0.296446
2.0	0.3503	0.35131	0.350137

REFERENCES

[1] S.U.S. Choi, "Enhancing thermal conductivity of fluids with nanoparticles", *ASME Fluids Engng. Div.* vol. 231, pp. 99-105, 1995.

[2] C.Y. Cheng, "Free convection boundary layer flow over a horizontal cylinder of elliptic cross section in porous media saturated by a nanofluid:, *Int. Commun. Heat Mass Transfer* vol. 39, pp. 931-936, 2012.

[3] A. Mahdy, S.E. Ahmed, "Laminar free convection over a vertical wavy surface embedded in a porous medium saturated with a nanofluid", *Transport Porous Media* vol. 91, pp. 423-435, 2012.

[4] Y.Q. Li, F.C. Wang, H. Liu, H.A. Wu, "Nanoparticle-tuned spreading behavior of nanofluid droplets on the solid substrate", *Microfluid Nanofluid* vol. 18, pp. 111-120, 2015.

[5] J. Sarkar, "A critical review on convective heat transfer correlations of nanofluids", *Renew Sust. Energ. Rev.* vol. 15, pp. 3271-3277, 2011.

[6] J. Buongiorno, "Convective transport in nanofluids", *J. Heat Transfer* vol. 128, pp. 240-250, 2006.

[7] O.D. Makinde, A. Aziz, "Boundary layer flow of a nanofluid past a stretching sheet with a convective boundary condition", *Int. J. Therm. Sci.* vol. 50, pp. 1326-1332, 2011.

[8] A. Mahdy, A.J. Chamkha, "Heat transfer and fluid flow of a non-Newtonian nanofluid over an unsteady contracting cylinder employing Buongiorno's model", *Int. J. Numer. Methods Heat & Fluid Flow* vol. 25(4), pp. 703-723, 2015.

[9] A. Mahdy, "Aspects of homogeneous-heterogeneous reactions on natural convection flow of micropolar fluid past a permeable cone", *App. Math. Comput.* vol. 352, pp. 59-67, 2019.

[10] A.J. Chamkha, R.S.R. Gorla, K. Ghodeswar, "Nonsimilar solution for natural convective boundary layer flow over a sphere embedded in a porous medium saturated with a nanofluid", *Transport Porous Media* vol. 86(1), pp. 13-22, 2010.

[11] S. Choi, "Nanofluids: from vision to reality through research", *J. Heat Transfer* vol. 131(3), pp. 1-9, 2009.

[12] A. Mahdy, "Natural convection boundary layer flow due to gyrotactic microorganisms about a vertical cone in porous media saturated by a nanofluid", *J. Braz. Soc. Mech. Sci. Engin.*, vol. 38(1), pp. 67-76, 2016.

[13] E.A. Sameh, A. Mahdy, "Natural convection flow and heat transfer enhancement of a nanofluid past a truncated cone with magnetic field effect", *World J. Mech.* vol. 2, pp. 272-279, 2012.

[14] E. Abu-Nada, H.F. Oztop, I. Pop, "Buoyancy induced flow in a nanofluid filled enclosure partially exposed to forced convection", *Superlattices Microstructures* vol. 51(3), pp. 381-395, 2012.

[15] C. Kleinstreuer, Y. Feng, "Experimental and theoretical studies of nanofluid thermal conductivity enhancement: a review", *Nano. Res. Lett.* vol. 6, pp. 1-13, 2011.

[16] A. Mahdy, M.E. Hillal, "Uncertainties in physical property effects on viscous flow and heat transfer over a nonlinearly stretching sheet with nanofluids", *Int. Commun. Heat Mass Transfer* vol. 39, pp. 713-719, 2012.

[17] A.V. Kuznetsov, D.A. Nield, "Natural convective boundary-layer flow of a nanofluid past a vertical plate", *Int. J. Therm. Sci.* vol. 49, pp. 243-247, 2010

[18] T. Hayat, M. Shafique, A. Tanveer, A. Alsaedi, "Magnetohydrodynamic effects on peristaltic flow of hyperbolic tangent nanofluid with slip conditions and Joule heating in an inclined channel", *Int. J. Heat Mass Transfer* vol. 102, pp. 54-63, 2016.

[19] T. Hayat, A. Shafiq, A. Alsaedi, "Characteristics of magnetic field and melting heat transfer in stagnation point flow of Tangent hyperbolic liquid", *J. Magn. Magn. Mater.* vol. 405, pp. 97-106, 2016.

[20] S.A. Shehzad, Z. Abdullah, F.M. Abbasi, T. Hayat, A. Alsaedi, "Magnetic field effect in three-dimensional flow of an Oldroyd-B nanofluid over a radiative surface", *J. Magn. Magn. Mater.* vol. 399, pp. 97-108, 2016.

[21] M. Waqas, T. Hayat, M. Farooq, S.A. Shehzad, A. Alsaedi, "Cattaneo-Christov heat flux model for flow of variable thermal conductivity generalized Burgers fluid", *J. Mol. Liq.* vol. 220, pp. 642-648, 2016.

[22] M.A. Abbas, Y.Q. Bai, M.M. Bhatti, M.M. Rashidi, "Three dimensional peristaltic flow of hyperbolic tangent fluid in nonuniform channel having flexible walls", *Alex. Eng. J.* vol. 55, pp. 653-662, 2016.

[23] F.S. Ibrahim, S.M. Abdel-Gaid, R.S.R. Gorla, "Non-Darcy mixed convection fl ow along a vertical plate embedded in a non-Newtonian fluid saturated porous medium with surface mass transfer", *Int. J. Numer. Meth. Heat & Fluid Flow* vol. 10, pp. 397-408, 2000.

[24] A. Mahdy, "Non-Newtonian nanofluid free convection flow subject to mixed thermal boundary conditions about a vertical cone", *J. Braz. Soc. Mech. Sci. Eng.* vol. 35, pp. 951-960, 2014.

[25] H.T. Chen, C.K. Chen, "Natural convection of a non-Newtonian fluid about a horizontal cylinder and a sphere in a porous medium", *Int. Commun. Heat Mass Transfer* vol. 15, pp. 605-614, 1988.

[26] H.T. Chen, C.K. Chen, "Free convection flow of non-Newtonian fluids along a vertical plate embedded in a porous medium", *ASME J. Heat Transfer* vol. 110, pp. 257-260. 1988.

[27] T. Salahuddin, M.Y. Malik, A. Hussain, M. Awais, I. Khanb, M. Khan, "Analysis of tangent hyperbolic nanofluid impinging on a stretching cylinder near the stagnation point", *Results in Physics* vol. 7, pp. 426-434, 2017.

[28] G.K. Ramesh, B.J. Gireesha, T. Hayat, A. Alsaedi, "Stagnation point flow of Maxwell fluid towards a permeable surface in the presence of nanoparticles", *Alex. Eng. J.* vol. 55, pp. 857-865, 2016.

[29] K.A. Yih, "Effect of radiation on natural convection about a truncated cone", *Int. J. Heat Mass Transfer* vol. 42, pp. 4299-4305, 1999.

[30] I. Pop, T.Y. Na, "Coupled heat and mass transfer by natural convection about a truncated cone in the presence of magnetic field and radiation effects", *Numer. Heat Transfer* Part A Application vol. 39, pp. 511-530, 2001.

[31] T.Y. Na, J.P. Chiou, "Laminar natural convection over a frustum of a cone", *App. Sci. Res.* vol. 35, pp. 409-421, 1979.

[32] R.S.R. Gorla, W.R. Schoren, H.S. Takhar, "Natural convection boundary layer flow of a micropolar fluid over an isothermal cone", *Acta Mech.* vol. 61, pp. 139-152, 1986.

[33] C.Y. Cheng, "Natural convection boundary layer flow of a micropolar fluid over a vertical per- meable cone with variable wall temperature", *Int. Commun. Heat Mass Transfer* vol. 38, pp. 429-433, 2011.

[34] A. Postelnicu, "Free convection about a vertical frustum of a cone in a micropolar fluid", *Int. J. Engng. Sci.* vol. 44, pp. 672-682, 2006.

[35] M.A. Hossain, C.S. Paul, "Free convection from a vertical permeable circular cone with non-uniform surface temperature", *Acta Mech.* vol. 151, pp. 103-114, 2011.

[36] F.G. Blottner, "Finite-difference methods of solution of the boundary-layer equation", *AIAA J.* vol. 8, pp. 193-205, 1970.

[37] R. Jawad, M.R. Azizah, O. Zurni, "Numerical investigation of copper-water (Cu-water) nanofluid with different shapes of nanoparticles in a channel with stretching wall: slip effects", *Math. Comput. Appl.* vol. 21, pp. 43-58, 2016.

[38] B.C. Pak, Y.I. Cho, "Hydrodynamic and heat transfer study of dispersed fluid with submicron metallic oxide particles", *Exper. Heat Transfer* vol. 11(2), pp. 151-170, 1998.

[39] L. Godson, B. Raja, D.M. Lal, S. Wongwises, "Experimental investigation on the thermal conductivity and viscosity of silver-deionized water nanofluid", *Exper. Heat Transfer* vol. 23(4), pp. 317-332, 2010.

[40] S.M. Aminossadati, B. Ghasemi, "Natural convection cooling of a localised heat source at the bottom of a nanofluid-filled enclosure", *Europ. J. Mech. B/Fluids* vol. 28(5), pp. 630-640, 2009.